

Strain Gradients in Epitaxial Ferroelectrics

G. Catalan^{1,*}, B. Noheda¹, J. McAneney², L. Sinnamon², and J. M. Gregg²

¹*Materials Science Center, University of Groningen, Groningen 9747AG, Netherlands and*

²*Department of Pure and Applied Physics, Queen's University Belfast, Belfast BT7 1NN, UK*

(Dated: November 18, 2004)

X-ray analysis of ferroelectric thin layers of $\text{Ba}_{1/2}\text{Sr}_{1/2}\text{TiO}_3$ with different thickness reveals the presence of internal strain gradients across the film thickness and allows us to propose a functional form for the internal strain profile. We use this to calculate the direct influence of strain gradient, through flexoelectric coupling, on the degradation of the ferroelectric properties of thin films with decreasing thickness, in excellent agreement with the observed behaviour. This work highlights the link between strain relaxation and strain gradients in epitaxial films, and shows the pressing need to avoid strain gradients in order to obtain thin ferroelectrics with bulk-like properties.

PACS numbers: 77.55.+f, 77.80.-e, 68.55.-a, 61.10.-i

The interest in ferroelectric thin films is rapidly expanding due to the recent development of both experimental techniques and calculation tools that allow to explore the ferroelectric phenomena at atomic level [1, 2]. The incorporation of realistic mechanical and electrical boundary conditions in the first-principles formulations is generating new insight on the mechanisms limiting the ferroelectric response in thin ferroelectric layers [3, 4, 5]. But while the new evidence suggests that ferroelectricity may indeed be stable in thin films only a few monolayers thick [1, 2, 3], the sharp peak in dielectric constant usually associated with the ferroelectric transition is systematically depressed in thin films. This obviously limits the technological impact that would arise from the ability to maintain ferroelectricity and large dielectric constants down to the nanoscale in real devices.

Strain caused by lattice mismatch with the substrate is an important factor affecting the properties of thin films. Strain can modify the phase diagram of epitaxial ferroelectrics [6, 7], change the order of the transition [7, 8], and shift transition temperatures [7, 9]. However, strain alone does not generally account for the observed smearing of the dielectric peak, as a sharp anomaly is still expected at the strain-modified transition temperature. Gradient terms (of strain, composition, defects, etc) have recently been proposed to account for the reduced dielectric constant [10, 11]. However, no experimental studies have provided quantitative insight in the gradient terms. The aim of the present work is to detect and measure strain gradients in a set of lattice-mismatched epitaxial thin films, and to correlate the measured gradients with the measured dielectric properties. The tools used in this work can be applied to any material where gradients, not just of strain but also of impurities or vacancies, are expected play a role. Showing the link between strain relaxation and strain gradients has therefore wider implications beyond ferroelectricity and is an important result for general thin film epitaxy.

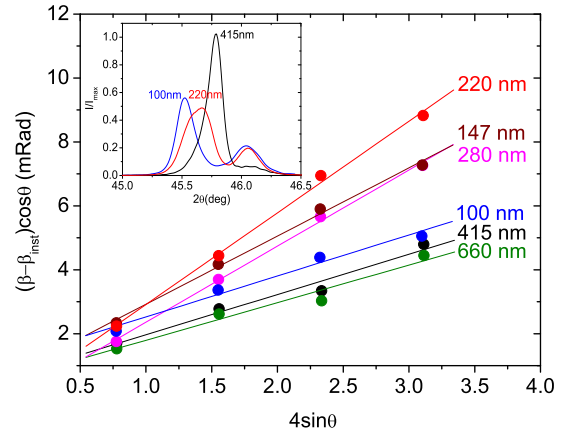


FIG. 1: (Color) Williamson-Hall plots as a function of film thickness. Inset: Diffraction peaks show that broadening is maximum at intermediate thickness. The peaks at 46.1 deg. correspond to the electrode (SRO)

The films studied in this work are $\text{Ba}_{0.5}\text{Sr}_{0.5}\text{TiO}_3$ (BST) dielectric layers with SrRuO_3 (SRO) bottom electrodes, grown by pulsed laser deposition. Epitaxy has been verified by cross-sectional high-resolution transmission electron microscopy (TEM). Details of the growth and TEM characterisation are published elsewhere [9]. In the present work the crystallographic analysis has been performed using a Philips X'pert MRD diffractometer with $\text{CuK}\alpha_1$ radiation ($\lambda=1.540 \text{ \AA}$).

The lattice parameters are extracted from the position of the perovskite pseudocubic (002) diffraction peak (see inset of Figure 1). This allows the calculation of the average out-of-plane strain in each film, given by $\bar{\epsilon}(t) = \frac{\bar{c}(t) - c_0}{c_0}$, where \bar{c} is the average out-of-plane lattice parameter, c_0 is the reference value, i.e., the bulk lattice parameter ($c_{\text{BST}} = 3.95 \text{ \AA}$), and t is the film thickness. The average strain for each film is shown in the inset of Figure 2. There is an out-of-plane expansion for the

*Electronic address: g.catalan@chem.rug.nl

thinnest films that decreases with thickness, as observed before [9, 12]. This is consistent with relaxation of the in-plane compression induced by the smaller lattice parameter of the bottom electrode ($c_{SRO} = 3.93 \text{ \AA}$).

Similar to what is known for semiconductor and metallic epitaxial layers, perovskite oxides are known to relieve strain as film thickness is increased. The strain-relieving mechanism is thought to be mainly the formation of misfit dislocations. As thickness increases, the accumulation of elastic strain energy overcomes the barrier for the formation of misfit dislocations, which ease the strain. It is generally implied that this strain relaxation is homogeneous across the film, and thus the strain state is only a function of the film's total thickness: $\epsilon = \epsilon(t)$.

However, around a dislocation the lattice is locally distorted. The accumulation of misfit dislocations at the film-substrate interface means that the film's lattice parameters are more distorted near the clamped surface than at the free one, leading to stress/strain distributions [12, 13, 14, 15]. Furthermore, strain may not be relaxed solely by dislocations, as other inhomogeneous mechanisms (such as vertical segregation of different-sized cations) have been observed [16]. Thus, rather than a quantity dependent only on the thickness t , strain should be described as an internal profile dependent also on the distance to the film-substrate interface, z : $\epsilon = \epsilon(z, t)$.

The homogeneous vs inhomogeneous scenarios of strain relaxation are not only different from a structural point of view, but have consequences for the functional properties. Inhomogeneous strain fields around dislocations [13, 14] and impurities [17] affect the polarisation and critical temperatures of ferroelectric thin films. Crucially, also, inhomogeneous strain is necessarily associated with local strain gradients, which couple to the polarisation via the flexoelectric effect [18, 19, 20]. Measuring the vertical strain gradient is therefore essential to correctly describe the functional properties of ferroelectric thin films.

In order to calculate the strain gradients, x-ray diffraction peak broadening has been analysed as a function of film thickness. There are at least two contributions to peak broadening: one due to the finite thickness of the sample, and another due to the inhomogeneous strain. The two have different angular dependence, and can therefore be separated by looking at peak width for different reflections and fitting the results using the Williamson-Hall relation [21]:

$$\beta \cos \theta = K \frac{\lambda}{D} + 4\epsilon_i \sin(\theta). \quad (1)$$

where D is the coherent length perpendicular to the film's surface (roughly proportional to the film's thickness), λ is the X-ray wavelength ($\lambda = 1.54 \text{ \AA}$ in our case), θ is the diffraction angle, β is the peak integral breadth (close to the full width half maximum) minus the instrumental broadening, and K is an empirical constant close to 1.

Linear fits of $\beta \cos \theta$ vs $\sin \theta$ yield the coherent length D and inhomogeneous strain ϵ_i for each film. We have performed such fits for the (00h) ($h=1:4$) reflections, find-

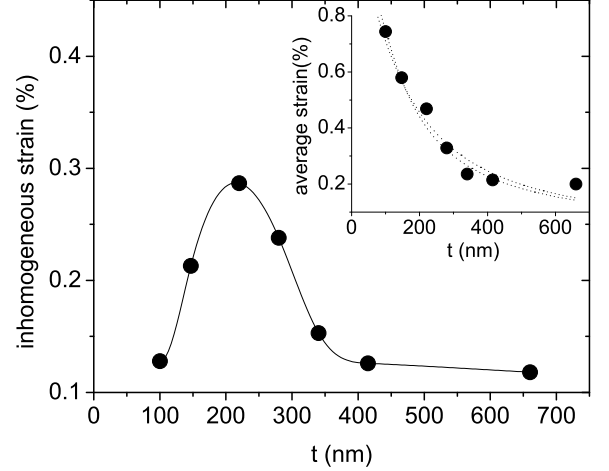


FIG. 2: Inhomogeneous strain as a function of film thickness. The solid line is a visual guide. Inset: average out-of-plane strain. Dotted lines are least-square fits using the averages of Eqs. 4 and 5.

ing the linear dependence excellent for all our samples ($r^2 > 0.9$) (Figure 1). It is nevertheless worth mentioning that the linear W-H plots are only one of existing strategies to separate size and strain broadening. Quantitative results for the inhomogeneous strain may therefore vary depending on the approach used [22].

Figure 2 shows the inhomogeneous strain as a function of film thickness. The existence of a maximum in ϵ_i confirms the presence of a monotonically decreasing internal strain profile as a function of z in the films. For very thin films the reduced thickness means a small dispersion in lattice parameters; conversely, for very thick films there may be a large difference between the lattice parameters at the clamped and free interfaces, but the volume fraction of totally relaxed material is large and dominates the diffraction, so that again the variance is small. In between, there is an intermediate thickness where there is a large dispersion in lattice parameters, with their thickness fractions being similar. At this point the inhomogeneous strain is maximum.

Establishing the actual mechanism of strain relaxation is beyond the scope of this paper, but it is worth mentioning that the observed behaviour is consistent with predictions for dislocation-based relaxation: the diffraction peak width in this case is expected to be proportional to $\sqrt{\rho/t}$, where ρ is the linear dislocation density, which grows rapidly around a critical thickness and then saturates [23].

Extracting quantitative values for the internal strain profile from this analysis requires solving the integral equations for the average ($\bar{\epsilon}$) and inhomogeneous (ϵ_i)

strain:

$$\bar{\epsilon}(t) = \frac{1}{t} \int_0^t \epsilon(z, t) dz, \quad (2)$$

$$\epsilon_i^2 = \frac{1}{t} \int_0^t [\epsilon^2(z, t) - \bar{\epsilon}^2(t)] dz = \bar{\epsilon}^2 - \bar{\epsilon}^2 \quad (3)$$

where $\bar{\epsilon}$, ϵ_i are extracted from peak position and width, respectively, and $\epsilon(z, t) = \frac{c(z, t) - c_0}{c_0}$ is the internal strain profile.

The easiest way to resolve these equations is the inverse approach: assume a certain shape for the internal strain, solve the integrals (2), (3), and modify the functional parameters to achieve a good match with the experimental results. This method relies heavily on the correct choice of functional dependence for $\epsilon(z, t)$. As such, the results of the quantitative analysis should be treated only as approximations.

A general model for the strain profile, independent of the actual relaxation mechanism, reflects that strain relaxation should be proportional to the strain itself, which yields an exponential dependence on z [24]:

$$\frac{\partial \epsilon}{\partial z} = -\frac{\epsilon}{\delta} \implies \epsilon(z) = \epsilon_0 e^{-\frac{z}{\delta}} \quad (4)$$

where ϵ_0 is the strain at the film-substrate interface, and δ is a measure of the penetration depth of the strain. If dislocations are considered as the main relaxation mechanism, a recent strain-gradient theory [15] predicts the vertical profile in the layers to be given by

$$\epsilon(z, t) = \epsilon_0 \left[\cosh \frac{z}{\delta} - \tanh \frac{t}{\delta} \sinh \frac{z}{\delta} \right] \quad (5)$$

It is worth noticing that Eq. (4) is a limiting case of (5) when the film thickness is larger than the strain penetration depth ($t \gg \delta$).

Either of these expressions can be integrated to yield $\bar{\epsilon}(t)$. The least-squares fits to the experimental results using both are shown as dashed lines in the inset of figure 1. The value of the fitting parameters is $\epsilon_0 = 0.013 \pm 0.001$ and $\delta = 60 \pm 12$ nm, and $\epsilon_0 = 0.010 \pm 0.001$ and $\delta = 85 \pm 13$ nm for the fits with the averages of (4) and (5) respectively.

The calculated curves for ϵ_i , using the above parameters also reproduce the experimental results for the maximum value and associated thickness. However, beyond the maximum, the predicted relaxation of ϵ_i using these equations is slower than experimentally measured. This discrepancy may be explained by the presence of more than one relaxation mechanism, each with different penetration length δ . Furthermore, ϵ_0 is a function of t , since the increase in dislocation density for thicker films affects the strain at the film-substrate interface. Thus, both parameters should, in principle, be considered as thickness-dependent: $\epsilon_0(t)$, $\delta(t)$. In order to calculate the thickness dependence of $\epsilon_0(t)$ and $\delta(t)$ we note that there are two parameters and two equations to describe $\bar{\epsilon}$ and ϵ_i , so it is possible to calculate ϵ_0 and δ for each film separately. We have done this for the exponential strain profile (4). Combining the Eqs. (2) and (3) we can eliminate ϵ_0 :

$$\frac{t}{2\delta} \frac{\bar{\epsilon}^2(t)}{(\epsilon_i^2 + \bar{\epsilon}^2)} = \tanh \left(\frac{t}{2\delta} \right) \quad (6)$$

This is solved for each film in order to find $\delta(t)$, which is then used to calculate $\epsilon_0(t)$.

Once the internal strain profile $\epsilon(z, t)$ is known, the strain gradient contribution to the functional properties can be calculated using an elastodielectric free energy expansion incorporating the flexoelectric contribution:

$$G = \int_0^t \left[\frac{1}{2} a P^2 + \frac{1}{4} b P^4 - \frac{1}{2} (s_{11} + s_{12}) \sigma^2 - Q_{13} \sigma P^2 - \gamma P \frac{\partial \sigma}{\partial z} - \eta \sigma \frac{\partial P}{\partial z} + \frac{1}{2} C \left(\frac{\partial P}{\partial z} \right)^2 + D \left(\frac{\partial \sigma}{\partial z} \right)^2 \right] dz \quad (7)$$

where P is the out-of-plane polarisation; s_{ij} the elastic compliances; σ the in-plane stress (related to the measured out-of-plane strain by the Young's modulus and Poisson's ratio: $\sigma = \epsilon Y(-2\nu)$); Q_{13} is the transverse electrostrictive coefficient, C and D are the constants related to the energy contributions from polarisation and stress gradient, and γ and ν are, respectively, the direct and converse flexoelectric coefficients. P is calculated by minimising the thermodynamic potential, while the second derivative of G with respect to P yields the inverse permittivity. This is averaged over the thickness of the film

to yield the effective value. The values of the coefficients used in this expansion are the same as in [10].

The relative dielectric constants calculated using the strain gradient extracted from our crystallographic analysis are shown in Fig.(2), along with experimentally measured for the same set of films. The predicted and measured temperatures of maximum permittivity (T_m) are shown in the inset.

Clearly, the decrease in dielectric constant and upward shift of T_m are well reproduced. Quantitatively, the prediction for T_m as a function of thickness is re-

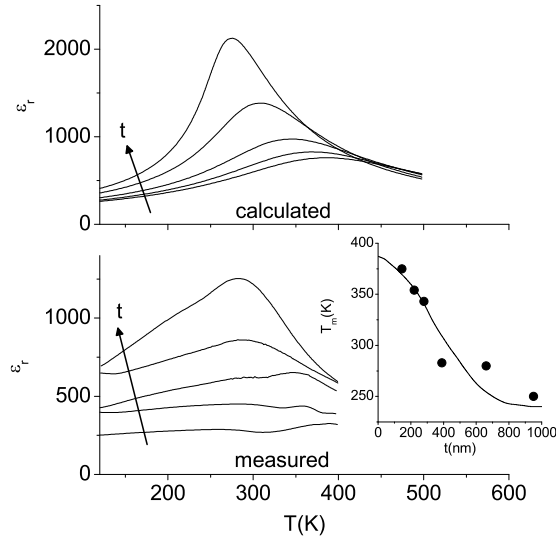


FIG. 3: Calculated and measured relative dielectric constant as a function of temperature for films of thickness 660 nm, 340nm, 280nm, 220nm and 145nm. Inset: Temperature of maximum permittivity, experimental (dots) and calculated (solid line)

markably good, while the calculated dielectric constant is larger than experimentally measured. This was expected, as our model does not take into consideration any other permittivity-depressing factors. The results show

that the contribution to the depression in permittivity with decreasing thickness (size effect) from flexoelectricity alone is enormous. This is particularly valid when compared with the huge permittivities recently measured in gradient-free ferroelectric films [25].

It is worth noting that the dielectric constant is lowest for the thinnest films in spite of the relatively small value of ϵ_i . This is a natural consequence of the fact that the size effect is *not* caused by the inhomogeneous strain itself, but by the strain gradient, which is largest for the thinnest films. We emphasise also that while compressive in-plane strain can indeed be used to stabilise the ferroelectric state, this may come at the expense of reducing the permittivity if strain gradients are not avoided. Also, the procedure outlined here could be used to estimate vertical oxygen vacancy distributions, or gradients due to impurity concentration. Finally, these methods open the scope for studying the effect of strain gradients on other functional materials.

In summary, X-ray analysis of peak broadening as a function of thickness shows that relaxation of strain in epitaxial films is associated with the appearance of internal strain gradients. The dielectric constants calculated using these strain gradients are close to experimentally measured, clearly showing the fundamental role played by flexoelectric coupling in decreasing the dielectric constant. This work shows the urgent need to avoid strain gradients in order to prevent degradation of the ferroelectric response in thin films.

Useful discussions with T. Hibma, E. Van der Giessen, T. Palstra and D. Boer are gratefully acknowledged.

-
- [1] R. Ramesh and D.G. Schlom, *Science* **296**, 1975 (2002).
 - [2] C.H. Ahn, K.M. Rabe and J-M Triscone *Science* **303**, 489 (2004) and refs therein.
 - [3] J. Junquera, P. Ghosez, *Nature* **422**, 506 (2003).
 - [4] I. Kornev, H. Fu, L. Bellaiche, *Phys. Rev. Lett.* **93**, 196104 (2004).
 - [5] C. Bungaro, K.M. Rabe, arXiv:cond-mat/0410375.
 - [6] O. Dieguez *et al.* *Phys. Rev. B* **69**, 212101 (2004).
 - [7] N. A. Pertsev, A. G. Zembilgotov, A. K. Tagantsev, *Phys. Rev. Lett.* **80**, 1988 (1998)
 - [8] C. Basceri, S. K. Streiffer, A. I. Kingon, R. Wasser, *J. Appl. Phys.* **82**, 2497 (1997)
 - [9] L. Sinnamon, R.M. Bowman, J.M. Gregg *Appl. Phys. Lett.* **81**, 889 (2002).
 - [10] G. Catalan, L. Sinamon, M. Gregg, *J. Phys. Cond. Mat.* **16**, 2253 (2004).
 - [11] A. M. Bratkovsky, A. P. Levanyuk, arXiv: cond-mat/0402100 (2004).
 - [12] C.L.Canedy *et al.* *Appl. Phys. Lett.* **77**, 1695 (2000).
 - [13] M.-W. Chu *et al.* *Nature Materials* **3**, 87 (2004).
 - [14] S. P. Alpay, I. B. Misirliglu, V. Nagarajan, R. Ramesh, *Appl. Phys. Lett.* **85**, 2044 (2004).
 - [15] L. Nicola, E. Van der Giessen, M. E. Gurtin, submitted to *J. Mech. Phys. Solids*.
 - [16] J.-L. Maurice *et al.*, *Phil. Mag.* **83**, 3201 (2003).
 - [17] D. Balzar, P. A. Ramakrishnan, A. M. Hermann, *Phys. Rev. B* **70**, 92103 (2004).
 - [18] Sh. M. Kogan, *Sov. Phys.Solid State*, **5** 2069 (1964)
 - [19] W. Ma, L.E. Cross *Appl. Phys. Lett.* **79**, 4420 (2001); *ibid* **81**, 3440 (2002)
 - [20] A. K. Tagantsev *Phys. Rev. B* **34**, 5883 (1986).
 - [21] G. K. Williamson, W. H. Hall, *Acta Metall.* **1**, 22 (1953).
 - [22] J. G. M. Van Berkum, R. Delhez, Th. H. De Keijser and E. J. Mittemeijer, *Acta Cryst. A* **52**, 730 (1996).
 - [23] V. M. Kaganer, R. Kohler, M. Schmidbauer, R. Opitz, B. Jenichen, *Phys. Rev. B* **55**, 1793 (1997).
 - [24] H. Joon Kim, S. Hoon Oh, Hyun M. Hang, *Appl. Phys. Lett.* **75**, 3195 (1999).
 - [25] M. M. Saad *et al.*, *J. Phys.: Cond. Mat.* **16**, 451 (2004).